



Hall effect and electrical conductivity studies of some MHD and fuel cell related materials
by Stuart Cody Snyder

A thesis submitted in partial fulfillment of the requirements for the degree of MASTER OF SCIENCE
in Physics

Montana State University

© Copyright by Stuart Cody Snyder (1978)

Abstract:

Hall effect and electrical conductivity studies were made on La_{0.95}Mg_{0.05}Al_{0.25}Cr_{0.75}O₃, La_{0.84}Sr_{0.16}CrO₃ and MgCr₂O₄, Hall effect studies were made on solid unseeded Rosebud ash coal slag, and two solid synthetic potassium seeded slags designated as NBS K-509 and NBS K-517. Temperatures ranged from 200°C to 950°C. Conductivity measurements were made in both air and argon atmospheres. Hall effect measurements were made only in argon atmospheres. Trial Hall effect measurements were made on mercury at room temperature without success. However, preliminary Hall effect measurements made at room temperature on a commercial Hall generator chip, and α -Fe₂O₃ on at temperatures from 200° to 600°C were successful. Experimental difficulties prevented conclusive Hall effect measurements in the slag, lanthanum chromite, and magnesium chromite samples. However, the Hall mobility of unseeded Rosebud slag was found to be less than 0.01 cm²/V-sec. at 925°C. The upper limit for the Hall mobility of La_{0.95}Mg_{0.05}Al_{0.25}Cr_{0.75}O₃ was found to be 0.07 cm²/V-sec. at 100°C, and for La_{0.84}Sr_{0.16}CrO₃, the upper limit is 0.2 cm²/V-sec. at 304°C. A.C. and D.C. electrical conductivity measurements of the lanthanum chromite based ceramics were in excellent agreement, indicating electronic conductivity. The measurements on MgCr₂O₄ indicate it is an ionic conductor.

STATEMENT OF PERMISSION TO COPY

In presenting this thesis in partial fulfillment of the requirements for an advanced degree at Montana State University, I agree that the Library shall make it freely available for inspection. I further agree that permission for extensive copying of this thesis for scholarly purposes may be granted by my major professor, or, in his absence, by the Director of Libraries. It is understood that any copying or publication of this thesis for financial gain shall not be allowed without my written permission.

Signature

Stuart C. Snyder

Date

July 25, 1978

Habe nun, ach, Philosophie,
Juristerei und Medizin
und leider auch Theologie
durchaus studiert, mit heißem Bemühn.
Da steh' ich nun, ich armer Tor
und bin so klug als wie zuvor!

Faust Part I Scène 1

by Johann Wolfgang von Goethe

HALL EFFECT AND ELECTRICAL CONDUCTIVITY STUDIES OF SOME

MHD AND FUEL CELL RELATED MATERIALS

by

STUART CODY SNYDER

A thesis submitted in partial fulfillment
of the requirements for the degree

of

MASTER OF SCIENCE

in

Physics

Approved:

V. Hugo Schmidt
Chairman, Graduate Committee

Robert J. Sorenson
Head, Major Department

Henry L. Parsons
Graduate Dean

MONTANA STATE UNIVERSITY
Bozeman, Montana

July, 1978

ACKNOWLEDGEMENTS

It is not possible to express my gratitude to those who made this thesis possible in a simple acknowledgement; nevertheless, I will try. A special thanks goes to Mark Baldwin, who not only built the Hall apparatus, but generously gave on many occasions his time and expertise. I am grateful to Al Belding for designing and building the voltage amplifier used, and for his advice in general. Dr. Masayoshi Yamada's help was greatly appreciated. My deepest thanks go to Dr. Hugo Schmidt and Dr. Surendra Sharma, whose guidance, assistance, criticism, and patience made this work a richly rewarding experience. Finally, I would like to thank my mother, who in addition to all she has done for me, typed the rough draft of my thesis, and Heidi Karsky, for typing the final draft.

TABLE OF CONTENTS

	Page
VITA	ii
ACKNOWLEDGMENT	iii
LIST OF TABLES	v
LIST OF FIGURES	vi
ABSTRACT	vii
INTRODUCTION	1
APPARATUS AND EXPERIMENTAL	20
EXPERIMENTAL RESULTS	40
CONCLUSIONS	57
REFERENCES	59

LIST OF TABLES

Table	Page
1. The Compositions of Rosebud Ash and the Synthetic Slags NBS-509 and NBS-517	43

LIST OF FIGURES

Figure	Page
1. Schematic of Furnace	23
2. Hall Electrode Configurations for Liquid and Solid Samples	27
3. Schematic of Balance Circuits	32
4. Schematic of Reference Output Voltage Amplifier . . .	34
5. Block Diagram of Hall Effect Experiment	35
6. Block Diagram of Electrical Conductivity Experiment .	37
7. The Hall Effect in $\alpha\text{-Fe}_2\text{O}_3$	47
8. Electrical Conductivity of $\text{La}_{.95}\text{Mg}_{.05}\text{Al}_{.25}\text{Cr}_{.75}\text{O}_3$ vs. Reciprocal Temperature in Air and Argon Atmospheres	49
9. Electrical Conductivity of $\text{La}_{.84}\text{Sr}_{.16}\text{CrO}_3$ vs. Reciprocal Temperature in an Argon Atmosphere	52
10. Electrical Conductivity of MgCr_2O_4 vs. Reciprocal Temperature in Air and Argon Atmospheres	54

ABSTRACT

Hall effect and electrical conductivity studies were made on $\text{La}_{.95}\text{Mg}_{.05}\text{Al}_{.25}\text{Cr}_{.75}\text{O}_3$, $\text{La}_{.84}\text{Sr}_{.16}\text{CrO}_3$ and MgCr_2O_4 , and Hall effect studies were made on solid unseeded Rosebud ash coal slag, and two solid synthetic potassium seeded slags designated as NBS K-509 and NBS K-517. Temperatures ranged from 200°C to 950°C. Conductivity measurements were made in both air and argon atmospheres. Hall effect measurements were made only in argon atmospheres. Trial Hall effect measurements were made on mercury at room temperature without success. However, preliminary Hall effect measurements made at room temperature on a commercial Hall generator chip, and on $\alpha\text{-Fe}_2\text{O}_3$ at temperatures from 200° to 600°C were successful. Experimental difficulties prevented conclusive Hall effect measurements in the slag, lanthanum chromite, and magnesium chromite samples. However, the Hall mobility of unseeded Rosebud slag was found to be less than 0.01 $\text{cm}^2/\text{V}\text{-sec.}$ at 925°C. The upper limit for the Hall mobility of $\text{La}_{.95}\text{Mg}_{.05}\text{Al}_{.25}\text{Cr}_{.75}\text{O}_3$ was found to be 0.07 $\text{cm}^2/\text{V}\text{-sec.}$ at 100°C, and for $\text{La}_{.84}\text{Sr}_{.16}\text{CrO}_3$, the upper limit is 0.2 $\text{cm}^2/\text{V}\text{-sec.}$ at 304°C. A.C. and D.C. electrical conductivity measurements of the lanthanum chromite based ceramics were in excellent agreement, indicating electronic conductivity. The measurements on MgCr_2O_4 indicate it is an ionic conductor.

INTRODUCTION

Development of coal-fired magnetohydrodynamics (MHD) and fuel cell electrical power generators is of great importance in providing for future energy needs. In developing these sources of electrical power, difficult materials problems are encountered and must be solved if these programs are to succeed. Research on the physical properties of certain materials considered for use in coal-fired MHD systems and high temperature solid electrolyte fuel cells is therefore vital. Accordingly, the purpose of this work was to study the electrical conduction process in some MHD and fuel cell related materials.

In a coal-fired MHD generator, high temperature plasma produced from the combustion of powdered coal passes between the poles of a superconducting magnet. A Lorentz force acts on the charged particles in the plasma and causes a current to flow transverse to the applied magnetic field. Magnetic viscosity, a frictional force which tends to prevent fluid flow in the direction perpendicular to the lines of magnetic force, opposes the motion of the plasma through the magnetic field, so it is necessary to produce a pressure gradient along the length of the channel to maintain the flow of the plasma. Hence, the expanding gas does work against the magnetic field. The electrical power generated by an MHD generator is therefore derived from the internal energy of the plasma. A series of segmented electrodes lining the walls of the MHD channel deliver the generated current to an external load.

An unwanted, yet unavoidable, by-product of a coal-fired MHD generator is coal slag. During operation the walls of the MHD channel are coated with a layer of molten slag approximately 2 mm thick. The slag must consequently have a high enough electrical conductivity so that MHD power generation is feasible, yet not so high as to short out the electrodes. The electronic conductivity of the plasma must be enhanced by seeding the slag with K_2CO_3 , K_2O or Cs_2CO_3 ; however, the addition of alkali metal ions makes molten slag corrosive to electrode materials. The electrode material therefore must be of high electrical conductivity and must be able to withstand corrosive slag at temperatures in excess of $1600^\circ C$. A thorough technical discussion of MHD can be found in the book by R. Rosa.¹

A fuel cell is essentially a continuously fueled chemical battery. One type of fuel cell (high temperature solid electrolyte fuel cell) under development is a device in which a reducing atmosphere of H_2 and CO produced by passing steam over burning charcoal, is separated from air by a solid electrolyte such as Cr doped ZrO_2 . The fuel cell generates electricity and gives off as by-products heat, oxygen deficient air and exhaust gases containing CO_2 , H_2O , and some CO . The typical fuel cell of this type operates around $1000^\circ C$, and generates voltages of about 1 volt. Therefore, many fuel cells must be connected in series with a suitable high temperature ceramic.

The materials considered for interelectrode connectors and MHD electrodes must be mechanically strong and have high electronic conductivity at high temperatures. Furthermore, MHD electrodes must be resistant to highly corrosive seeded slags. Materials under strong consideration for use as interconnecting electrodes and MHD electrodes are the lanthanum chromite based ceramics. Also magnesium chromite is a possible MHD electrode material. Lanthanum chromite with alkaline earth ions generally enhances the mechanical strength and electrical conductivity of this ceramic.²

To state the objective of our work explicitly, we are concerned with investigating the electrical conduction processes of the lanthanum chromite based ceramics $\text{La}_{.95}\text{Mg}_{.05}\text{Al}_{.25}\text{Cr}_{.75}\text{O}_3$ and $\text{La}_{.84}\text{Sr}_{.16}\text{CrO}_3$, magnesium chromite, and potassium seed coal slag by determining the temperature dependence of the current carrier density, electrical conductivity, and the nature (electrons, holes, or ions) and sign of the current carrier. Electrical conductivity studies of some seeded slags were made by Pollina³ and will not be repeated by us. The temperature range of interest is from 200 to 300°C to temperatures in excess of 1600°C. Slag samples are liquid at the higher temperatures (above 1200°C).

The Hall effect provides a rather simple way, in principal at least, of determining the concentration of current carriers in a material, the sign of the current carrier, and whether or not

conduction is ionic or electronic in nature. It was first observed by E. H. Hall in 1879, that when a current flows through a material in the presence of a transverse magnetic field, an electric field develops that is transverse to both the current and the applied magnetic field. The force on the current carriers that results from the magnetic field causes them to migrate to the surface of the material. The transverse electric field that results produces a force on the current carriers that opposes the force due to the magnetic field. Equilibrium occurs when the force due to the transverse, or Hall field, balances the magnetic force. The magnitude of the Hall voltage is dependent upon the electrical conductivity of the material and on the concentration of current carriers. The sign of the Hall voltage gives the sign of the current carrier.

Limited information about current carriers, namely the sign of the carrier, can be obtained from the Seebeck effect. The Seebeck effect is a thermoelectric effect first observed in 1822. When two different materials are joined together to form a complete circuit, and the two junctions of the circuit are held at different temperatures, a thermal electromotive force between the two junctions is generated. Charges migrate from the hot junction to the cold junction until the resulting electric field becomes large enough to stop the migration. The polarity of the junctions indicates whether the carriers are positive or negative.

A thermoelectric effect that is analogous to the Hall effect and yields the same information as the Hall effect is the Nernst effect. If instead of an applied current, a temperature gradient is established along a material in the presence of a transverse magnetic field, the migrating charges will be deflected and an electric field perpendicular to the temperature gradient and magnetic field will be established. The Nernst effect is a possible source of error in doing Hall effect measurements if there exists a temperature gradient along the direction of the applied current.

Further thermoelectric effects that can be mistaken for Hall voltages are the Ettingshausen and Righi-Leduc effects. If the current carriers moving through a material all had the same velocity, their trajectories in a magnetic field would all be the same. In reality the carriers have a velocity distribution. As a result, the trajectories of the higher velocity carriers curve less sharply than the trajectories of the lower velocity carriers. This has the effect of distributing higher energy (hotter) carriers on one side of the material, and lower energy (colder) carriers on the opposite side, as dictated by the magnetic field direction. This distribution sets up a temperature gradient and produces a Seebeck thermoelectric field perpendicular to the applied electric field and magnetic field. This is known as the Ettingshausen effect. If the current through the sample results from a temperature gradient instead of an applied electric field, this

phenomenon is called the Righi-Leduc effect. At any rate, these effects can give rise to apparent Hall voltages and are a potential source of error.

The following simple physical model affords us a reasonably accurate mathematical description of the Hall effect. This model is discussed in many standard textbooks on solid state physics. The model considers a statistical distribution of current carriers, electrons for example, as essentially free particles moving within the material. After some time, an individual electron will collide with some lattice imperfection, phonon, or impurity. We assume the electron loses all of its kinetic energy during the collision, and that the electron's motion is completely random before and after a collision. Since we are discussing a statistical distribution of electrons, we can think of a mean free time between collisions. In other words, an electron averages one collision every τ seconds, where τ is the mean free time. The mean free time is considered to be a constant for a given temperature, electric or magnetic field, and composition of the sample studied.

In the presence of electric and magnetic fields, an electron experiences a Lorentz force given by

$$\vec{F} = -e(\vec{E} + \vec{v} \times \vec{B}) = M \frac{d\vec{v}}{dt} \quad (1)$$

where e is the magnitude of the electronic charge.

The current density in the x-direction produced by the i^{th} electron is

$$J_{ix} \hat{i} = \frac{-e v_x \hat{i}}{a_x A} \quad (2)$$

where A is the cross-sectional area of the sample, and a_x is some distance in the x-direction the electron travels. We can write the above as

$$J_{ix} \hat{i} = \frac{-e v_x \hat{i}}{V} \quad (3)$$

where V is the volume of the sample.

The current density in the other directions can likewise be written as

$$J_{iz} \hat{j} = \frac{-e v_z \hat{j}}{V} \quad (4)$$

and

$$J_{iz} \hat{k} = \frac{e v_z \hat{k}}{V}.$$

This gives the current density produced by the i^{th} electron as

$$\vec{J}_i = \frac{e \vec{v}_i}{V} \quad (5)$$

Equation (1) can be rewritten in terms of \vec{J}_i as

$$\frac{MV}{e} \frac{d\vec{J}_i}{dt} = e(\vec{E} + \frac{V}{e} \vec{J}_i \times \vec{B}). \quad (6)$$

This simplifies to

$$\frac{d\vec{J}_i}{dt} = \frac{e^2}{MV} \vec{E} + \frac{e \vec{J}_i \times \vec{B}}{M} \quad (7)$$

If we sum over all of the electrons, we have

$$\frac{d\vec{J}}{dt} = \frac{ne^2\vec{E}}{M} + \frac{e\vec{J}}{M} \times \vec{B} \quad (8)$$

with n being the number of electrons per unit volume (current carrier concentration). Equation (8) is the equation of motion of the current density in a material in the presence of electric and magnetic fields. In deriving equation (8), the effect of collisions with lattice imperfections and phonons has not been included. Since the mean free time of an electron is τ , the probability that a collision occurs in a time dt is $\frac{dt}{\tau}$. Therefore, the change in the current density in a time interval dt due to collisions is

$$d\vec{J}(t) = -\frac{dt}{\tau} \vec{J}(t). \quad (9)$$

It is assumed that τ is much less than the period of revolution of a free electron in a magnetic field. It is found experimentally⁷ that for a free electron in a magnetic field of 10 kG, the cyclotron frequency is $\omega_c = 1.8 \times 10^{11}$ rad/sec. Relaxation times for copper at room temperature are typically 2×10^{-14} sec., so $\omega_c \tau \approx 3.5 \times 10^{-3}$.

The net change in current density is found by adding equations (8) and (9). We get

$$\frac{d\vec{J}_{net}}{dt} = \frac{ne^2}{M} \vec{E} - \frac{e\vec{J}}{M} \times \vec{B} - \frac{\vec{J}}{\tau}. \quad (10)$$

Under steady state conditions, current density is constant in time,

so

$$\vec{J} = \frac{ne^2\tau}{M} \vec{E} - \frac{e\tau\vec{J}}{M} \times \vec{B}. \quad (11)$$

Consider the applied magnetic field in the z-direction. In component form, equation (11) becomes

$$\begin{aligned} J_x &= \frac{ne^2\tau}{M} E_x - \frac{e\tau}{M} BJ_y \\ J_y &= \frac{ne^2\tau}{M} E_y + \frac{e\tau}{M} J_x B \\ J_z &= \frac{ne^2\tau}{M} E_z. \end{aligned} \quad (12)$$

If the applied electric field is in the x-direction, in steady state conditions, current only flows in the x-direction, and we must have

$$J_y = 0$$

$$J_z = 0.$$

As a result of the above restrictions, equations (12) give

$$\begin{aligned} J_x &= \frac{ne^2\tau}{M} E_x \\ E_y &= \frac{-J_x B}{ne} \end{aligned} \quad (13)$$

$$E_z = 0.$$

We can make use of Ohm's law to simplify equations (13). Ohm's

law states

$$\vec{J} = \sigma \vec{E} \quad (14)$$

where σ is the conductivity of the material. As mentioned before (equation 3), the current density is

$$\vec{J} = -nev. \quad (15)$$

In an applied electric field, Newton's Second Law is

$$M \frac{d\vec{v}}{dt} = -e\vec{E}. \quad (16)$$

However, when the effect of collisions is added, the above equation is modified to

$$\frac{d\vec{v}}{dt} = \frac{\vec{v}}{\tau} - \frac{e\vec{E}}{M}. \quad (17)$$

Since \vec{J} is constant in time, \vec{v} is also constant in time, and we have from equation (17)

$$\vec{v}_D = \frac{e\vec{E}\tau}{M} \quad (18)$$

where \vec{v}_D is the drift velocity of the electron.

Using equation (18) in equations (15) and (14), we can write the conductivity as

$$\sigma = \frac{ne^2\tau}{M}. \quad (19)$$

We can now write equations (13) as

$$J_x = \sigma E_x$$

$$E_y = -\frac{\sigma E_x B}{ne}. \quad (20)$$

The electric field E_y is the Hall field. For a sample with a rectangular cross-section with the thickness dimension in the y-direction, the Hall voltage is found from equation (20) to be

$$V_H = E_y t = \frac{-\sigma E_x B t}{ne} \quad (21)$$

where t is the sample thickness.

The Hall voltage is measured in Hall effect experiments. It is, however, inconvenient to describe the Hall effect in terms of the Hall voltage, which depends on sample geometry, and applied electric and magnetic fields. Instead, one defines the Hall coefficient R as

$$R \equiv \pm \frac{E_y}{j_x B_z} = \pm \frac{1}{ne} \quad (22)$$

Measurement of the Hall coefficient gives the sign and concentration of the current carriers. A negative Hall coefficient means the majority of current carriers are electrons, while a positive Hall coefficient tells us the majority carriers are holes.

The conductivity of a sample can be written by combining equations (14) and (15) as

$$\sigma = ne \mu_D \quad (23)$$

where μ_D is the drift mobility, or the drift velocity divided by the applied electric field. Equation (22) allows us to define another constant, called the Hall mobility, as

$$\mu_H \equiv \sigma |R| = \mu_D \quad (24)$$

In general, the Hall mobility and drift mobility are not equal. According to the simple model we used in deriving the above mathematical description of the Hall effect, we assumed that the mean free time for all carriers was the same, and independent of the kinetic energy of the carriers. In reality, τ is a function of the carrier's energy, and the carriers are not all of the same energy but have energies distributed in the conduction band according to Fermi-Dirac statistics. When one takes this into account, and approaches the problem by considering the effect of a Lorentz force on the unperturbed Fermi-Dirac distribution function, it is found^{4,5} that

$$R \equiv \pm \frac{E_y}{j_x B_z} = \pm \frac{3\pi}{8} \frac{1}{ne} \quad (25)$$

This gives the result

$$\mu_H = \frac{3\pi}{8} \mu_D \quad (26)$$

in light of equation (24). One should not expect the Hall mobility to reduce to the drift mobility in the absence of a magnetic field; the Hall mobility is defined differently than the drift mobility.

Notice that the modification factor $3\pi/8$ is of the order one, so the mathematical description of the Hall effect we have developed based on our simple model is, to a first approximation, correct. Equations (25) and (26) are used when the samples studied are semiconductors. For metals and very impure semiconductors in which the electrons behave as

electrons in a metal, Shockley⁵ shows that $\mu_H = \mu_D$. This is because all conduction electrons in a metal have essentially the same kinetic energy.

In many cases, the charge carriers are both electrons and holes. When this is the case (intrinsic semiconductors, for example), the electrical conductivity becomes

$$\sigma = e(n\mu_n + p\mu_p) \quad (27)$$

where n and p are the electron and hole concentrations, respectively, and μ_n and μ_p the electron and hole mobilities, respectively.

The expression for the Hall coefficient becomes more complicated when two types of carriers are present. It can be shown⁵ that R becomes

$$R = \frac{p - nb^2}{(nb + p)^2 e} \quad (28)$$

where $b = \mu_n / \mu_p$.

If $p \approx n$ and $\mu_n \approx \mu_p$, equation (28) tells us that R is small, and consequently, the Hall voltage is small. Furthermore, the sign of the Hall coefficient can change over a temperature range as the mobilities μ_n and μ_p change relative to each other.

Because of their large mass, ions have relatively low mobilities. Consequently, the Hall effect in ionic conductors is difficult to accurately measure, and other means must be used to determine carrier concentrations and signs.⁶

Since our studies involve measuring electrical conductivities of materials over a temperature range, it is useful to derive an expression for conductivity as a function of temperature to help interpret experimental data.

According to the band theory of semiconductors, conduction can occur only if electrons occupy the conduction band. In intrinsic semiconductors, the conduction band is vacant at absolute zero. As the temperature increases, electrons are thermally excited from the valence band into the conduction band, leaving holes in the valence band which also contribute to the conduction process. To calculate the number of electrons in the conduction band as a function of temperature, gives an expression for conductivity as a function of temperature.

We assume the electrons in the conduction band to be a gas of essentially free electrons. The density of states for the electrons is

$$g(E) = \frac{1}{2\pi^2} \left(\frac{2M^*}{\hbar^2} \right)^{3/2} E^{1/2} \quad (29)$$

where M^* is the effective mass of the electron. The above equation comes from solving the free particle Schrödinger equation with periodic boundary conditions. Details can be found in standard textbooks on solid state physics, such as Kittel.⁷ If we take $E=0$ to be the top edge of the valence band we have

$$g(E) = \frac{1}{2\pi^2} \left(\frac{2M^*}{\hbar^2} \right)^{3/2} (E - E_g)^{1/2} \quad (30)$$

where E_g is the width of the band gap. The above equation is the density of states function for electrons with energies greater than or equal to bottom of the conduction band. The number of electrons per unit volume in the conduction band can be found using Fermi-Dirac statistics and the density of states function. We can write

$$N_e = \int_{E_g}^{\infty} g(E) n_e(E) dE \quad (31)$$

where $n_e(E)$ is the Fermi-Dirac distribution function. Explicitly,

$$n_e(E) = \frac{1}{1 + \exp \frac{(E - E_F)}{kT}} \quad (32)$$

The constant E_F is the Fermi energy, the highest energy state available to the electrons at absolute zero, and k is Boltzmann's constant. The number of electrons per unit volume in the conduction band is therefore

$$N_e(T) = 2 \left(\frac{2\pi M^* kT}{\hbar^2} \right)^{3/2} \exp \left(\frac{E - E_F}{kT} \right). \quad (33)$$

The number of holes per unit volume in the valence band is similarly calculated by using the distribution function for holes

$$M_h = 1 - M_e \quad (34)$$

where n_h is the probability that a state is occupied, and noting that the energy of holes increases downward from the top of the valence band, we get

$$N_h = 2 \left(\frac{2\pi M_h^* kT}{h^2} \right)^{3/2} \exp \left(\frac{-E_F}{kT} \right) \quad (35)$$

where we have assumed $\exp \left(\frac{E - E_F}{kT} \right) \gg 1$.

We can use our expressions for electron and hole densities in equation (27) to get an expression for conductivity as a function of temperature for an intrinsic semiconductor. Upon substitution, we get

$$\sigma = \sigma_0 \exp \left(\frac{-E_G}{2kT} \right) \quad (36)$$

where

$$\sigma_0 = 2|e| \left(\frac{2\pi kT}{h^2} \right)^{3/2} (M_e^* M_h^*)^{3/4} (\mu_n + \mu_h).$$

The energy $E_G/2$ is called the activation energy U of the conduction process. As can be seen by equation (36), the temperature dependence of conductivity is governed by an exponential factor. If one plots $\ln \sigma$ versus reciprocal temperature, the resulting graph is a straight line, and the slope of the line is proportional to the activation energy.

The addition of impurities to a crystal (called doping) can have a large effect on the conductivity. Impurity atoms can donate electrons to the conduction band, or accept electrons from neighboring atoms in the crystal, and create holes in the valence band. Energy levels are introduced into the band gap as a result of doping. Electrons occupying donor states near the conduction band are thermally activated into the conduction band, and electrons in the valence band are thermally excited into acceptor states lying near the top of the valence band and produce holes in the valence band. The result is an enhancement of electrical conductivity. Semiconductors of this type are called extrinsic. The electrical conductivity of extrinsic semiconductors has the same form as in intrinsic semiconductors. If we assume that only one type of carrier predominates (electrons for example) it is shown⁸ that

$$\sigma = \sigma_0 \exp\left(\frac{-E_D}{2kT}\right) \quad (37)$$

where

$$\sigma_0 = 2|e| \mu_n N_D \left(\frac{M_e^* kT}{2h^2}\right)^{3/2}$$

with N_D being the donor concentration. The quantity $E_D/2$ is the activation energy for conduction. The assumption that only one carrier predominates is reasonable because of the law of mass action,⁷ which

states that the product of electron and hole concentrations is constant for a given temperature. Therefore, if electrons are added by doping, the number of holes must decrease. In other words, doping with a donor suppresses conduction by holes, and likewise doping with acceptors suppresses conduction by electrons. At high temperatures, the number of carriers thermally excited into the conduction band far exceed the number of carriers due to impurities, and conduction enters the intrinsic range.

So far little has been said about ionic conductivity other than the fact that ions have low mobilities when compared with electrons or holes. The two chief ionic conduction mechanisms are migration of an ion from one interstitial site (Frenkel defect) to another, and hopping of an ion from an ion site to an adjacent ion vacancy site (Schottky defect). The temperature dependence of ionic conductivity is governed by the same exponential factor found in the expressions for electronic conductivity.⁸ In other words, we have

$$\sigma \propto \exp \left(\frac{-E_G}{2kT} \right) \quad (38)$$

with $E_G/2$ being the activation energy. Many ionic conductors have relatively large activation energies (around 6 eV),⁸ and consequently are poor conductors except at high temperatures. (Insulators typically have an activation energy of around 10 eV).

Special theoretical problems are encountered when one studies the electrical properties of amorphous semiconductors because of the lack of a periodic structure. Since some of our work involves amorphous materials, a brief qualitative description of conduction processes in this type of material will be given. An excellent reference that studies the properties of amorphous semiconductors in depth is by Mott and Davis.⁹ It turns out that the density of states for amorphous semiconductors is not too different from that for crystalline semiconductors. However, one expects to find a considerable difference between the Hall mobility and drift mobility. It can be shown¹⁰ that $\mu_H \ll \mu_D$ for the case of conduction by a thermally activated electron hopping from site to site.

APPARATUS AND EXPERIMENTAL METHOD

In designing a Hall effect apparatus, many things must be considered. Several different techniques to measure the Hall effect are available, the appropriate technique depending on the nature of the experiment and existing apparatus. One particular technique used to measure Hall mobilities is called the Corbino disk method. A radial current flows between the rim of a disk-shaped sample and the center of the sample in the presence of a magnetic field perpendicular to the face of the disk. A circular Hall current results. If the applied current is A.C., the Hall current is also A.C., and may be measured by a pick-up coil located near the sample. This method is described in detail by Carver¹¹ who successfully applied this technique to measuring Hall mobilities in amorphous semiconductors. This technique could be used with liquid samples, but it would require a vertical magnetic field which is impractical with our facilities.

The technique we used was chosen because of existing equipment in the laboratory; namely a large D. C. electromagnet capable of fields up to 13,000 gauss with a 5 inch air gap, and a Princeton Applied Research Model HR-8 Phase Sensitive Detector (lock-in) with a high impedance (10M) preamplifier. The HR-8 supplies an A.C. electric current that is transverse to the applied magnetic field. The resulting Hall voltage, which is at the same frequency as the reference voltage, is fed into the

HR-8, and the output is displayed on a chart recorder as a D.C. voltage.

The heart of the system is the lock-in amplifier, which can measure small signals that are buried in noise. The lock-in operates as follows. The signal fed into the preamplifier is multiplied by the reference, or output signal generated by the lock-in and integrated over the period of the signal. The result is a D.C. voltage which is displayed on a chart recorder and is proportional to the Hall voltage. In general, there is a phase difference between the input signal and the reference voltage. If the input signal is in phase with the reference signal, we get a maximum D.C. output. On the other hand, if the reference and input voltages are 90° out of phase, we get zero D.C. output. The lock-in lets us adjust the phase of the reference voltage to equal the phase of the input signal thus optimizing the D.C. output. Noise is filtered out of the lock-in output if the magnitude of the difference between the signal frequency and noise frequency is greater than the reciprocal of the output filter time constant. An example of the lock-in's operation might be helpful at this point. Consider one Hall electrode fed into terminal "A" of the preamplifier, and the other electrode fed into terminal "B". On the "A" minus "B" mode of operation (differential mode) the voltage that is mixed with the reference voltage is

$$V_S = 2V_H \sin (wt + \phi). \quad (39)$$

The product of the phase-adjusted reference voltage and the signal is

$$V_R V_S = 2A V_H \sin (wt + \phi) \sin (wt + \phi). \quad (40)$$

Upon integrating the above from 0 to $2\pi r$, we get the D.C. output voltage

$$V_{D.C.} = A V_H \quad (41)$$

where A is determined by calibrating the chart recorder.

Another advantage in using an A.C. applied voltage is that errors due to the Ettinghausen effect are eliminated. The other thermal-electric effects that can introduce error can be eliminated by assuring the sample is at a uniform temperature. Other spurious effects may be detected by periodically reversing the direction of the magnetic field. The D.C. output displayed on the chart recorder is shifted either above or below the zero magnetic field base line when the field is reversed. If the spurious effect does not depend on the direction of the magnetic field, it can be detected. A voltage produced by the Nernst effect for instance will not be detectable by this method. Other methods for detecting errors in Hall effect measurements are described in the literature.¹²

Because we are interested in high temperature measurements of the Hall effect, a furnace was designed that would fit between the pole caps of the magnet. See Figure 1 for a schematic drawing. The furnace

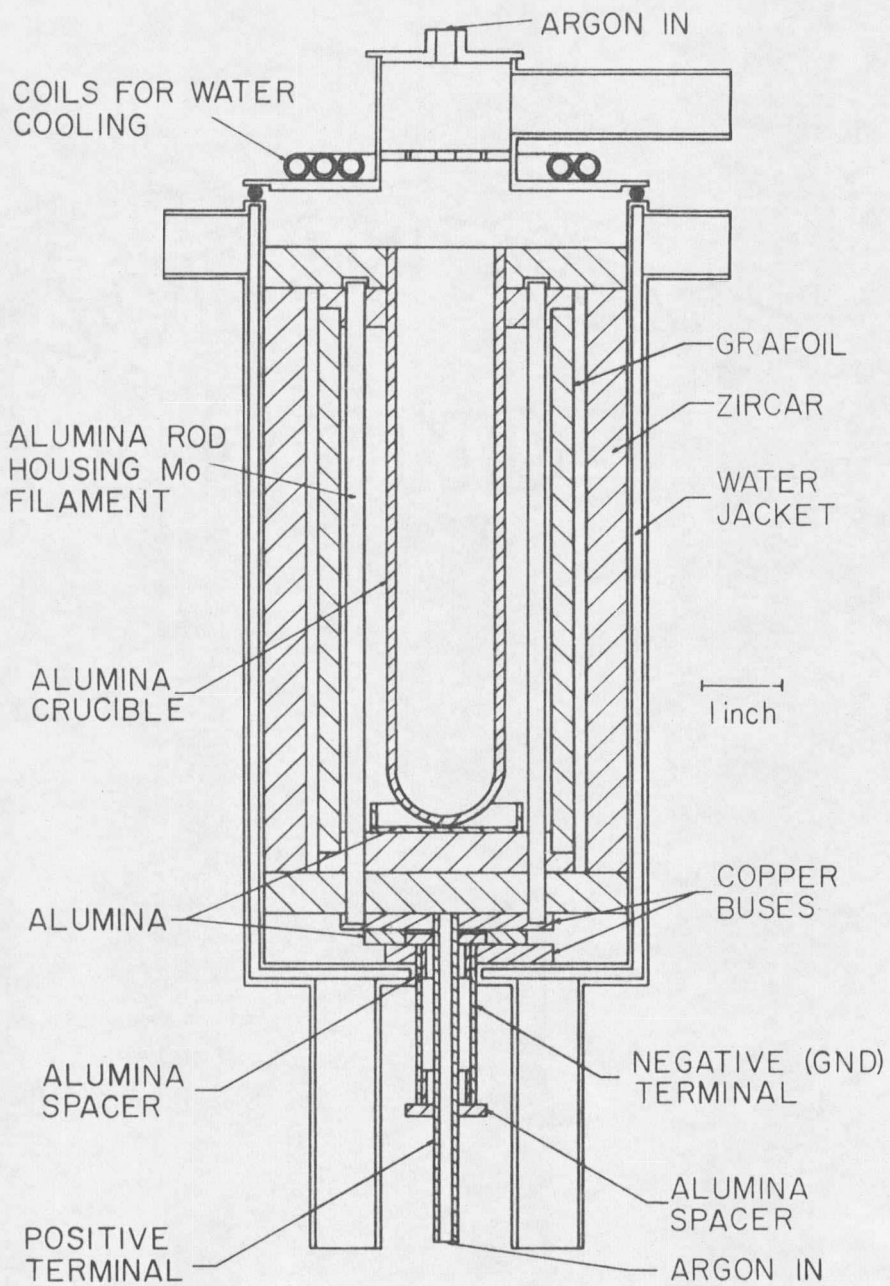


Figure 1. Schematic of Furnace

consists of a double-walled copper can with a removable copper lid. A steady flow of water from a large water tank is maintained in the space between the two walls in order to keep the exterior of the can cool and protect the magnet pole caps. The water tank provides a reservoir that will continue to cool the furnace in the event of line water failure. The lid is also cooled by water flowing through coiled copper tubes silver-soldered on to it. Inside the can are two layers of insulation. The first is a cylinder of Zircar zirconia fiber, manufactured by Zircar Products, Inc., 110 North Main St., Florida, NY 10921, and next is a cylinder of Grafoil thermal radiation-reflecting graphite supplied by Fiber Materials, Inc., Biddeford Industrial Park, Biddeford, MA 04005. These two layers of insulation help keep the power requirements of the heater to a minimum.

The heating element is an 11 ft. length of 50 mil molybdenum wire bent into eight tight hairpins, or inverted U's which are then equally spaced around a cylindrical alumina crucible.

Because the heater element carries a large current (~30 amps. D.C.) in the presence of high magnetic fields (~10kG), magnetic forces acting on the heater wire must be compensated for. This is achieved by running the molybdenum wire through one bore of a double bore alumina rod (20cm in length and 0.67cm in diameter), then doubling the wire back on itself and running it through the other bore. In this way, the compressive forces of the wire on a given alumina tube cancel and do not

tend to bend the tube. One end of the wire is connected to a copper bus in the bottom of the can, while the other end is attached to the can itself, which is grounded.

In winding the furnace in this method, the potential difference between adjacent heater wires (separated by about 1 mm of alumina) is minimized thereby reducing the chance of electrical breakdown at high temperatures of the alumina between the wires. This would result in shorting out the furnace. (This indeed happened with an earlier method of winding the furnace in which the end of the wire connected to the positive terminal and the end connected to the negative terminal were housed in the same alumina rod and electrical breakdown of the alumina occurred).

The crucible mentioned above acts as a cavity in which solid samples may be placed. The temperature within this cavity remains quite stable after thermal equilibrium has been reached. The crucible also serves as a sample holder for liquid samples.

To prevent problems caused by oxidation, ports are provided in the lid and bottom of the can to allow purified argon to flow in. Hence, all Hall effect measurements must be done on an argon atmosphere. On several earlier test runs, oxidation of the Grafoil insulation posed a problem. Viewing ports located in the side of the can let enough air get into the can to ruin the Grafoil. Air also leaked in from the top of the can because the lid was not properly sealed. These problems

